Complete Chemical Analysis of Aerosol Particles in Real-Time

Mo Yang, Peter T. A. Reilly, Reiner A. Gieray, William B. Whitten, J. Michael Ramsey

Oak Ridge National Laboratory, Chemical and Analytical Sciences Division
Oak Ridge, TN 37831-6142, USA

Abstract : Real-time mass spectrometry of individual aerosol particles using an ion trap mass spectrometer is described. The microparticles are sampled directly from the air by a particle inlet system into the vacuum chamber. An incoming particle is detected as it passes through two CW laser beams and a pulsed laser is triggered to intercept the particle for laser ablation ionization at the center of the ion trap. The produced ions are analyzed by the ion trap mass spectrometer. Ions of interest are selected and dissociated through collision with buffer gas atoms for further fragmentation analysis. Real-time chemical analyses of inorganic, organic, and bacterial aerosol particles have been demonstrated. It has been confirmed that the velocity and the size of the incoming particles highly correlate to each other. The performance of the inlet system, particle detection, and preliminary results are discussed.

1. Introduction

MASTER

An important aspect of environmental atmospheric monitoring requires the chemical characterization of airborne microparticles and aerosols. Some recent studies have correlated the health effects with the concentration of atmospheric particles/1,2/. Unfortunately, traditional sample collection and handling techniques are prone to contamination and interference effects that can render an chemical analysis invalid. These problems can be avoided by using real-time atmospheric sampling techniques followed by immediate mass spectrometric analysis. Several groups have reported advances in the use of laser desorption mass spectrometry

DISCLAIMER

DISCLAIMER

Portions of this document may be illegible
in electronic image products.   Images are
produced from the best available original
document.

(LDMS) to characterize individual airborne particles in real time/3-12/. While the laser ablation ionization can be used for the analysis of either organic or inorganic species, organic species are best characterized by tandem mass spectrometry because of the high degree of fragmentation and the large number of compounds with similar masses. Recently, tandem mass spectrometry on individual microparticles by laser ablation/ionization in an ion trap has been developed in this laboratory/13/ and applied to chemical analysis of aerosol particles, using a direct particle inlet system/14-16/. Detection limits appear to be well below a femtogram per particle. In addition to the primary and MS/MS analyses, information about the particle size estimated by velocity measurement enhances the specificity in the microparticle characterization. In this paper, the construction and performance of a reliable source of standard particles of known size and composition, the atmospheric particle interface, and a method for particle detection and laser triggering so that laser sampling occurs at the proper place and time are described. Various aspects of this real-time aerosol mass spectrometer are discussed with measured experimental results.

2. Experimental

2.1 Sampling interface

Figure 1 shows the principal diagram of the experimental setup. The particle inlet system consists of a 2 cm long 0.5 mm id capillary followed by 0.50 mm and 0.25 mm diameter skimmers. Two roughing pumps (pumping speed 500 L/min) and one turbo molecular pump (pumping speed 100 L/sec) served for evacuation of the two intermediate regions and the ion trap chamber. Approximately, 0.6 L of air entered the inlet system per minute. The ion trap chamber was filled with 1 mTorr of helium to optimize ion trapping and mass measurement.

2.2 Particle detection

Since the particles were accelerated to nearly the speed of sound, 150-400 m/s, and the laser output pulse is delayed from the input trigger pulse, the laser must be triggered prior to the arrival of particles at the ionization region. It was therefore necessary to sense the particles at two positions and measure the individual velocity of the particle. Two parallel CW laser beams were focussed at the axis of the apparatus, crossing the particle beam path.. The laser light

scattered by a particle was collected by optical fibers that lead to photomultiplier tubes located outside of the vacuum chamber. A block diagram of the electronic circuits needed to measure the particle velocity and to control the ion trap is shown in Figure 2. The Count Up and Count Down circuits ensured that time from the second beam to the trap center was proportional to the time between the two beams. The counters were driven by two different clock frequencies, which were set so that the ionization laser was triggered to fire when the particle arrives at trap center. The number of clock pulses that can be convoluted to the velocity was registered for each particle in a separate computer.

2.3 Sample particle generation

Two configurations of particle generator have been used. The first is based on a vibrating orifice liquid droplet generator that produces a stream of monodisperse droplets 10 to 50 um in diameter./17/ Solid particles are obtained by drying an aqueous solution of either the desired substance or a salt plus traces of the analyte. The particles are carried by airflow through a drying tube to the entrance aperture of the spectrometer interface. We have consistently been able to produce uniform particles of controlled size from potassium nitrate solutions in this way. The second system uses a Collison nebulizer instead of the vibrating orifice. The droplets produced are less uniform in size but the apparatus is less sensitive to clogging up. This system is used when solid particles are to be aerosolized. Particles can be coated by another analyte that is ted in solution.

2.4 Laser desorption ionization

The intial tests of the aerosol mass spectrometer were made with a Quanta-Ray Nd-YAG laser, operating on the third harmonic, at a wavelength of 355 nm. Double trigger pulses from the particle detection electronics were used for triggering the flash lamps and Q-switch so that the laser pulse intercepts the particle at the trap center. An Excimer laser (308 nm) was also used at higher duty cycle than 10-Hz Nd-YAG laser. While this laser has no flash lamps, constraints on the Thyratron still require double pulse triggering.

2.5 Ion trap mass spectrometer

Standard ion trap electrodes and electronics (Finnigan MAT, Model ITMS) were used in the experiment. The ring electrode has been modified by

drilling four holes for laser beam and particle beam introduction. Mass spectra of trapped ions were obtained by ramping the RF voltage on the ring electrode of the trap./18/ Positive ions were detected by a Channeltron multiplier placed behind a hole on the end cap electrode. Negative ions were detected indirectly by means of a conversion dynode near the Channeltron./19/ The ion trap control functions as if the trap were a mass selective detector for a gas chromatograph, running a cyclical scan consisting of the following segments: (1) an ionization period in which an electron gun is gated on and the trap conditions are set to store ions of a predetermined mass range, (2) a selection interval in which ions of particular m/z are isolated, (3) an interval for collision-induced dissociation (CID) in which the selected ions are fragmented, and (4) a mass scan in which the ions are ejected from the trap and detected in ascending order of m/z./20/ If only a primary mass spectrum is desired, the two central segments are omitted. Because laser ablation is being used to generate the ions, the electron gun is nornamlly disconnected by the measurement. However, the oneset of electron gun gate signal is used to latch the processor in the ITMS electronics in HALT mode until the ionization laser is triggered. Thus, the ion trap is in the ion storage condition at the time ions are generated and the desired mass spectrum will be acquired. After the data are stored, the control electronics package starts a new scan and is halted to await the next particle. Once the process is initiated, the system is free running, acquiring mass spectra of every particle that triggers the pulsed laser.

3. Results and Discussion

3.1 Particle size and velocity

The particle detection has been tested with various size of latex spheres. As shown in Figure 3, it has been found that the particle flight time between two detectors (21 mm) was linearly proportional to the particle size. For example, the particle size distribution of two different sizes (1.53 um and 3.46 um) convoluted from the measured flight time is shown in the upper left corner. This means that the aerodynamic size of an incoming particle can be individually determined by measuring the time-of-flight. This enables one to differentiate species of particles by flight time, similar to retention time in gas chromatography, prior to measuring the mass spectrum.

3.2 Isotope ratio

Figure 4 shows the measured mass spectrum of an airborne KNO₃ salt particle with a size of 15 um. The potassium isotope ratio (m/z 39 and 41) measured here was 6.9 % while the natural abundance is 6.7 %. This demonstrates that the isotope ratio of an element can be measured with a single microparticle directly from the air. This method can be applied, for example, to the monitoring of nuclear activities. If an unnatural isotope ratio of an element is detected from airborne dust particles, it could be a fission product and a signature of nuclear activity in that area.

3.3 Organic molecules

Figure 5 shows some measurements of cigarette smoke particles. The top is the primary spectrum of a smoke particle, the middle is isolation of the ions that appear at m/z 162, and the bottom one is the fragment spectrum dissociated from the isolated ions. From this fragmentation pattern, the parent ions at m/z 162 can be verified as nicotine. This indicates that unknown organic particles in the air can be completely analyzed in real-time as to molecular structure.

3.4 Bacteria

One of the most interesting applications of this method is real-time detection of biological particles, such as pollen, spores, viruses, and bacteria. Figure 6 shows a negative mass spectrum of airborne bacteria, *Bacillus subtilis.* MS/MS fragmentations were measured for several ion peaks. The loss of m/z 16 and 18 from the ions at m/z 79 and 97, respectively, supports the assignment of m/z 79 to PO₃⁻ and m/z 97 to H₂PO₄⁻. Many of the prominent ions, for example m/z 181, appear to be organophosphate ions since m/z 79 predominates in the MS/MS spectra. Figure 7 shows the size distribution and positive ion mass spectra of *Aerobacter aerogenes.* While most aerosolized bacteria appeared to consist mainly of single cells, a bimodal size distribution was observed for *Aerobacter aerogenes.* The characteristic pattern in the mass spectra was the same for both modes of size distribution. This indicates the presence of cell aggregates as well as single cells.

4. Conclusions

We have shown in this study that it is possible to characterize an aerosol particle as to its size and composition in real time. Structural information about

molecular species in individual airborne microparticles can be obtained through tandem mass spectrometry with an ion trap. A large number of ions can be produced from a single airborne microorganism and there are a number of prominent ions that appear in the mass spectrum. The presence of these ions may make possible a real-time single particle discriminator for microorganisms and particles of nonbiological origin.

Acknowledgement

References

1. J. Schwartz, *Environ. Res.*, 64, 36–52 (1994).
2. D. W. Dockery, J. Schwartz, J. D. Spengler, *Environ. Res.*, 59, 362–373 (1992).
3. B. C. Dionne, D. P. Rounbehler, E. K. Achter, J. R. Hobbs, D. H. Fine, *J. Energetic Mat.*, 4, 447–472 (1986).
4. M. P. Sinha, *Rev. Sci. Instrum.*, 55, 886–891 (1984).
5. P. J. McKeown, M. V. Johnston, D. M. Murphy, *Anal. Chem.*, 63, 2069–2073 (1991).
6. O. Kievit, J. C. M. Marijinissen, P. J. T. Verheijen, B. Scarlett, *J. Aerosol Sci.*, 23, Suppl. 1, S301–304 (1992).
7. D. M. Murphy, D. S. Thomson, *Aerosol Sci. Tech.*, 22, 237 (1995).
8. K. P. Hinz, R. Kaufmann, B. Spengler, *Anal. Chem.*, 66, 2071–2076 (1994).
9. K. A. Prather, T. Nordmeyer, K. Salt, *Anal. Chem.*, 66, 1403–1407 (1994).
10. T. Nordmeyer, K. A. Prather, *Anal. Chem.*, 66, 3530–3542 (1994).
11. P. G. Carson, K. R. Neubauer, M. V. Johnston, A. S. Wexler, *J. Aerosol Sci.*, 26, 535–545 (1995).
12. W. D. Reents, Jr., S. W. Downey, A. B. Emerson, A. M. Mujsce, A. J. Miller, D. J. Siconolfi, J. D. Sinclair, A. G. Swanson, *Aerosol. Sci. Tech.*, 23, 263–270 (1995).
13. M. Yang, J. M. Dale, W. B. Whitten, J. M. Ramsey, *Anal. Chem.*, 67, 4330–4334 (1995).
14. M. Yang, P. T. A. Reilly, K. B. Boraas, W. B. Whitten, J. M. Ramsey, *Rapid Commun. Mass Spectrom.*, 10, 347–351 (1996).
15. P. T. A. Reilly, R. A. Gieray, M. Yang, W. B. Whitten, J. M. Ramsey, *Anal. Chem.*, In printing.
16. R. A. Gieray, P. T. A. Reilly, M. Yang, W. B. Whitten, J. M. Ramsey, *Appl. Environ. Microbiology*, In printing.
17. R. N. Berglund, B. Y. H. Liu, *Environ. Sci. Technol.*, 7, 147–153 (1973).
18. G. C. Stafford, Jr., P. E. Kelly, J. E. P. Syka, W. E. Reynolds, J. F. J. Todd, *Int. J. Mass Spectrom. Ion Proc.*, 60, 85 (1984).
19. S. A. McLuckey, G. L. Glish, P. E. Kelley, *Anal. Chem.*, 59, 1670–1674 (1987).
20. S. A. McLuckey, G. L. Glish, G. J. Van Berkel, *Int. J. Mass Spectrom. Ion Proc.*, 106, 197 (1991).

Figure Captions

Figure 1   Schematic diagram of the experimental setup.

Figure 2   Block diagram of the electronics circuit that measures the particle velocity and controls the laser timing

Figure 3   Flight time vs. size for monodisperse latex spheres. The inset shows the measured size distribution for latex spheres of 1.53 um and 3.46 um diameter, respectively.

Figure 4   Mass spectrum of a KNO_3 particle (15 um) injected directly from the air into the ion trap.

Figure 5   Mass spectra of cigarette smoke. Top: primary mass spectrum. Middle: Isolation of ions at m/z 162. Bottom: MS/MS fragmentation spectrum of ions at m/z 162. The fragmentation pattern of nicotine is distinct.

Figure 6   Averaged negative ion mass spectrum of *B. subtilis*. The arrows indicate the daughter ions observed by dissociation of ions at m/z 79, 97, and 181.

Figure 7   Size distribution and averaged positive ion mass spectra of *Aerobacter aerogenes type I*. A bimodal distribution of particle size has been observed while the pattern of mass spectra are the same for the both sizes.

AIRBORNE PARTICULATE

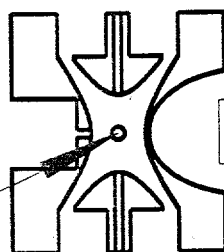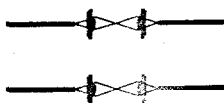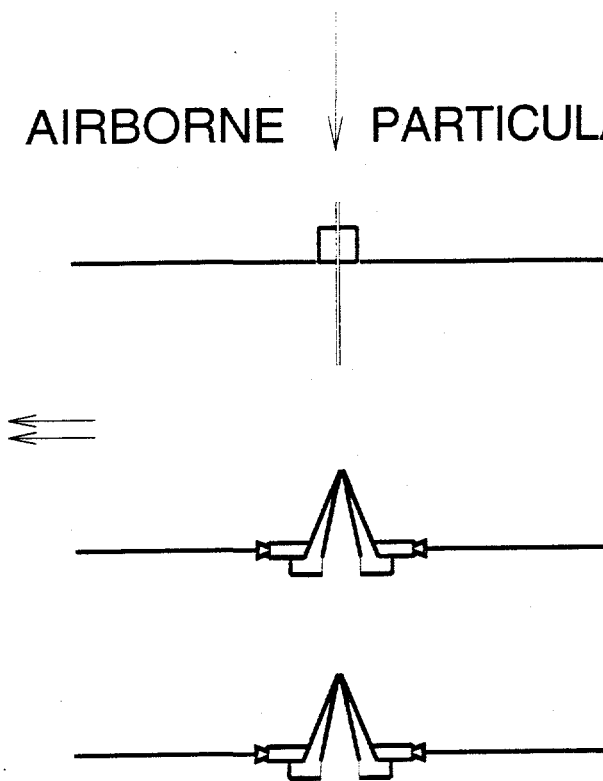DIFFERENTIAL
PUMPING

CW ION LASER $\quad\Longrightarrow$ PMT1
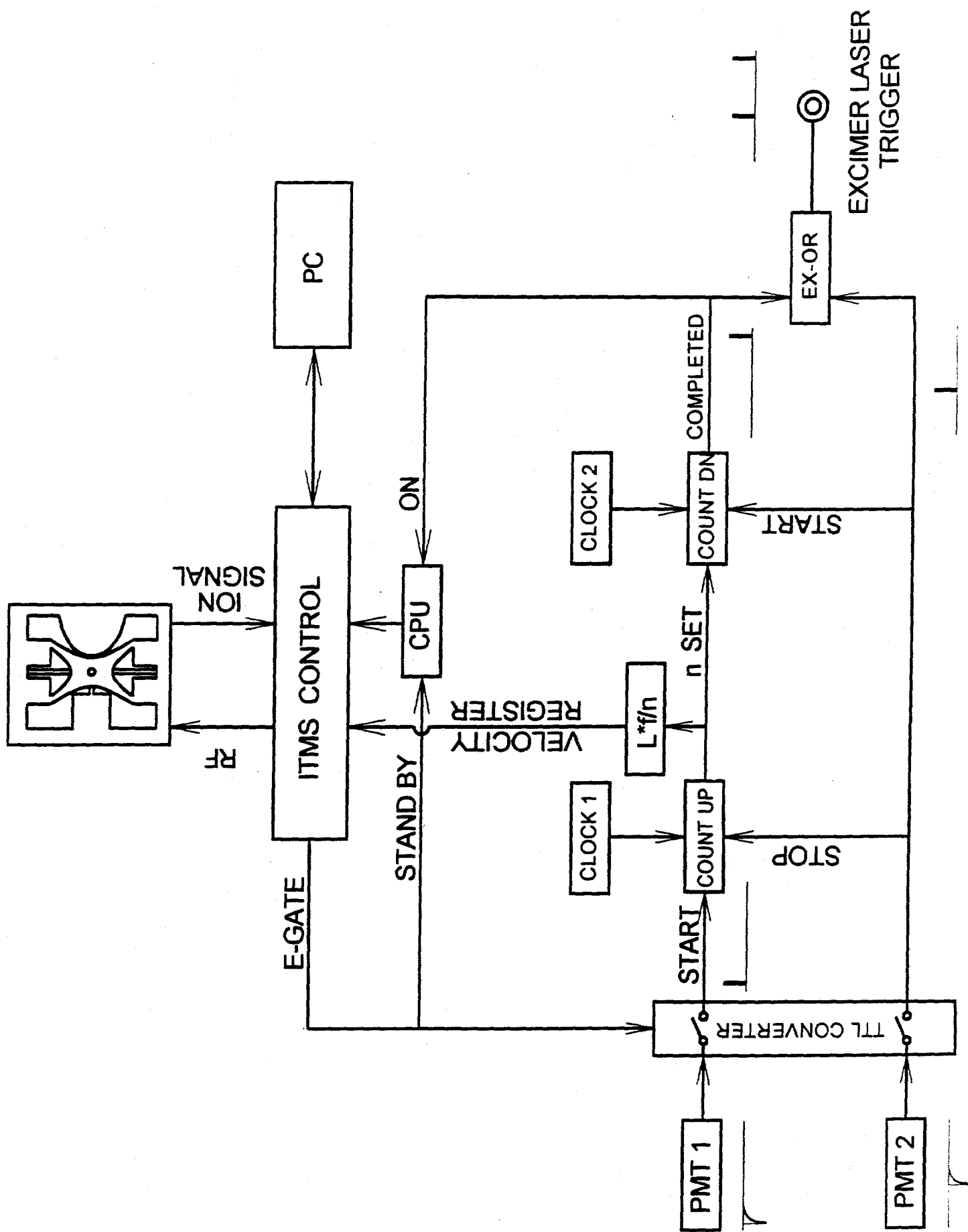
$\Longrightarrow$ PMT2

CHANNELTRON
ION DETECTOR

DESORPTION
LASER

ITMS

Main plot axes:
- x-axis: aerodynamic diameter / μm (0 to 10)
- y-axis: flight time / μs (50 to 100)

Inset plot axes:
- x-axis: aerodyn. diameter / μm (0.5 to 5)
- y-axis: number of particles (0 to 150)
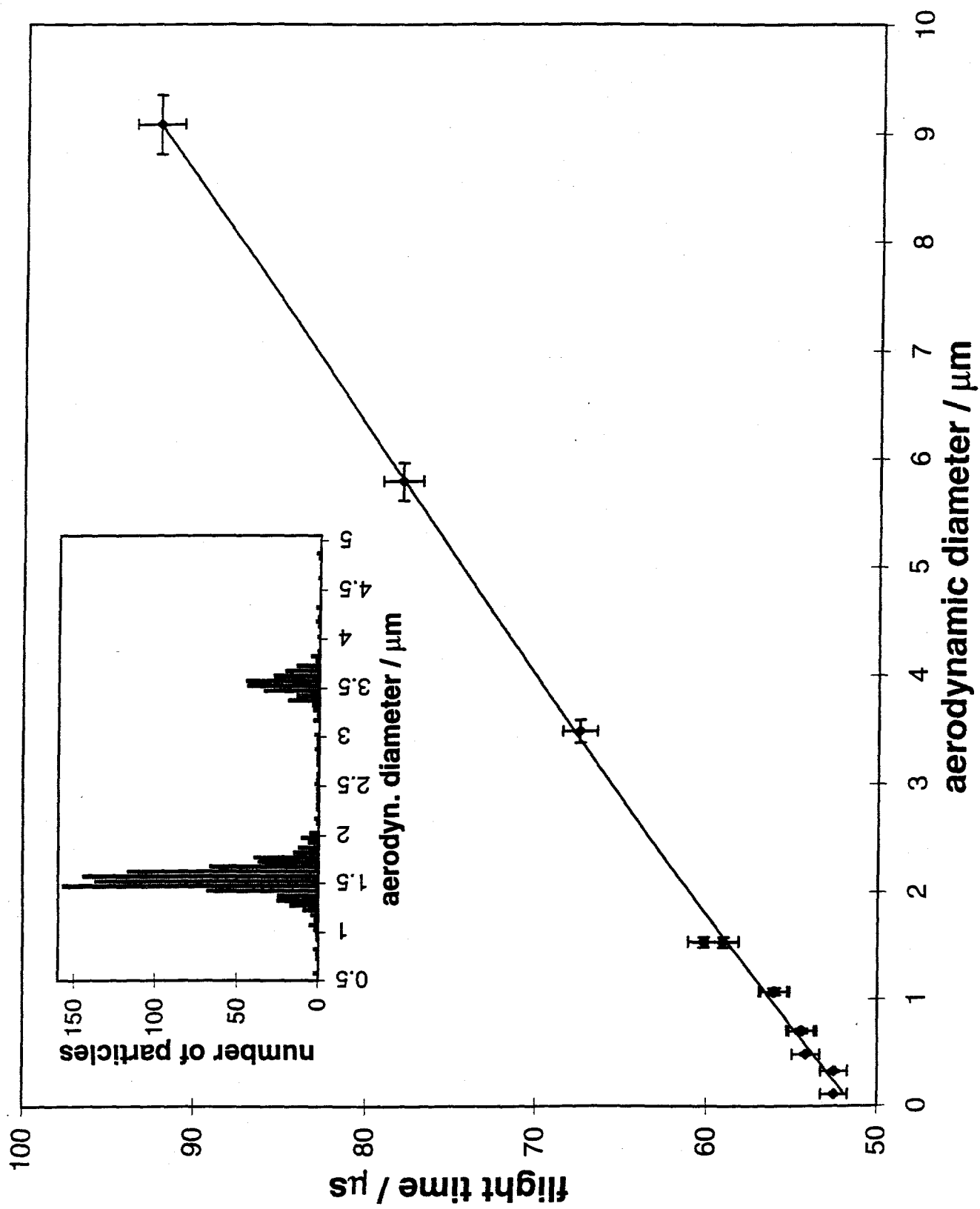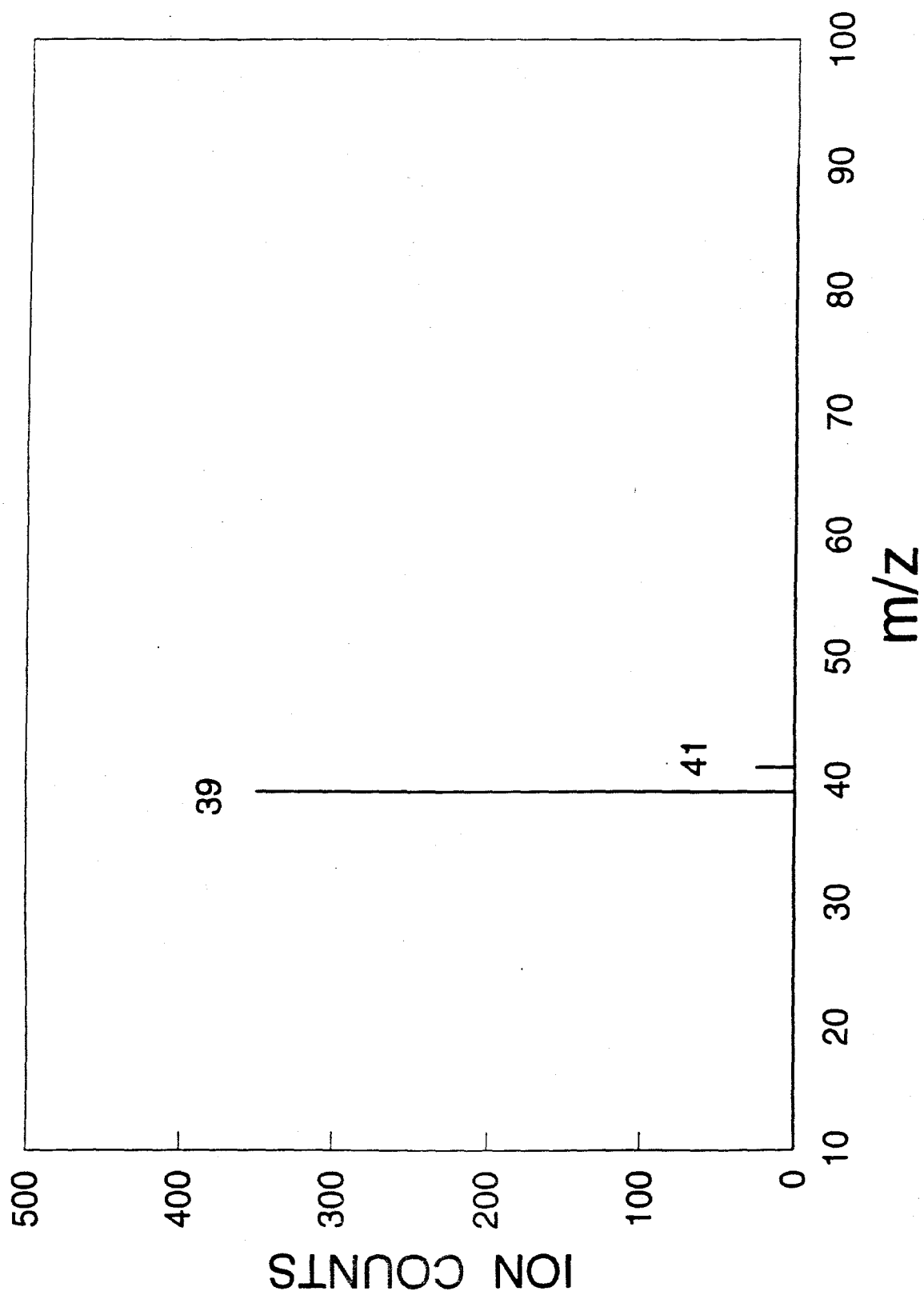
Nicotine in Cigarette Smoke

Bacillus subtilis

—— MS/MS

63
79
97
153
159
181
199 215
241
261 277

m/z

intensity (arb. units)

100000
80000
60000
40000
20000
0

50   100   150   200   250   300   350

particles < 1.5 μm

particles > 1.5 μm

Size distribution of
Aerobacter aerogenes

intensity (arb. units)

m/z

m/z

number of particles

aerodynamic diameter / μm